QUINTANA SOMALIA

INTERPRETATION AND OPERATIONS REPORT OF AN AEROMAGNETIC SURVEY OF PART OF THE SOMALI REPUBLIC

QUINTANA SOMALIA LIMITED

INTERPRETATION AND OPERATIONS REPORT

OF AN AEROMAGNETIC SURVEY

OF A PART OF THE

SOMALI REPUBLIC

Hunting Geology and Geophysics Ltd.
Elstree Way,
Borehamwood WD6 1SB
Hertfordshire,
England.

Tel: 01 953 6161
Telex: 23517 A/B HUNBOR G
Cables: ASTEREO BOREHAMWOOD

Contract No. 210 166
February 1982.

CONTENTS

CONTENTS

PART 2 - OPERATIONS REPORT

APPENDICES

FIGURES

SUMMARY

A high sensitivity aeromagnetic survey of part of the Somali Republic was flown for Quintana Somalia Limited between mid-July and mid-November, 1981. The survey totalled 14,419 line km of flying and data were acquired at three heights (3,500 ft, 4,500 ft and 6,000 ft above sea level), in four blocks. The eastern area was flown with a 4 x 8 km grid and the western area with a 3 x 6 km grid. Flight lines were orientated north - south, with east - west tie lines.

This report is in two parts:

Part 1, the Interpretation Report, briefly outlines the geological background and describes the aeromagnetic data and their interpretation.

Part 2, the Operations Report, describes the survey operation and the acquisition and compilation of the data.

Four basement zones have been recognised, each displaying a series of major basement depressions and areas of uplift.

To the west a major basin reaching -6.9 km (below sea-level), trends east - west and is thought to reflect the Red Sea Trend.

In Zone 2, basement is generally less magnetic than in other parts and no strong structural trend is seen.

Zone 3 exhibits strong basement structures associated with both Red Sea and Gulf of Aden Trends. They form a series of troughs and ridges, ranging from 0.8 km to -2.3 km in depth.

The geophysical coverage over Zone 4 is less than over the other zones and only one major basin has been located in the extreme eastern part of the survey area which exceeds - 3.5 km in depth.

A good correlation is shown between interpreted structure and other available data. Some recommendations for futher geophysical investigation are made.

PART 1

INTERPRETATION REPORT

1. INTRODUCTION

A high-sensitivity aeromagnetic survey was flown by Hunting Geology and Geophysics Limited between mid-July and mid-November, 1981, over the concession held by Quintana Somalia Limited in northern Somalia.

The survey objective was to assist in the delineation of areas of potential hydrocarbon resources by determining basement structure and areas of maximum thickness of sedimentary section.

Part 1 of this report describes the interpretation of the aeromagnetic data. The flying operations and compilation procedures are described in Part 2, the Operations Report.

The location map and sheet layout are shown in Text Figure 1, which also indicates the zones of differing flying height.

The aeromagnetic survey statistics are as follows:

Total line kilometres flown	14,419 km
Date flying commenced	14th July 1981
Crew stand-down (due to weather)	12th August - 1st October 1981
Date flying completed	13th November 1981
Flight line orientation	North - South
Tie line orientation	East - West
Flight line spacing	3 or 4 km
Tie line spacing	6 or 8 km

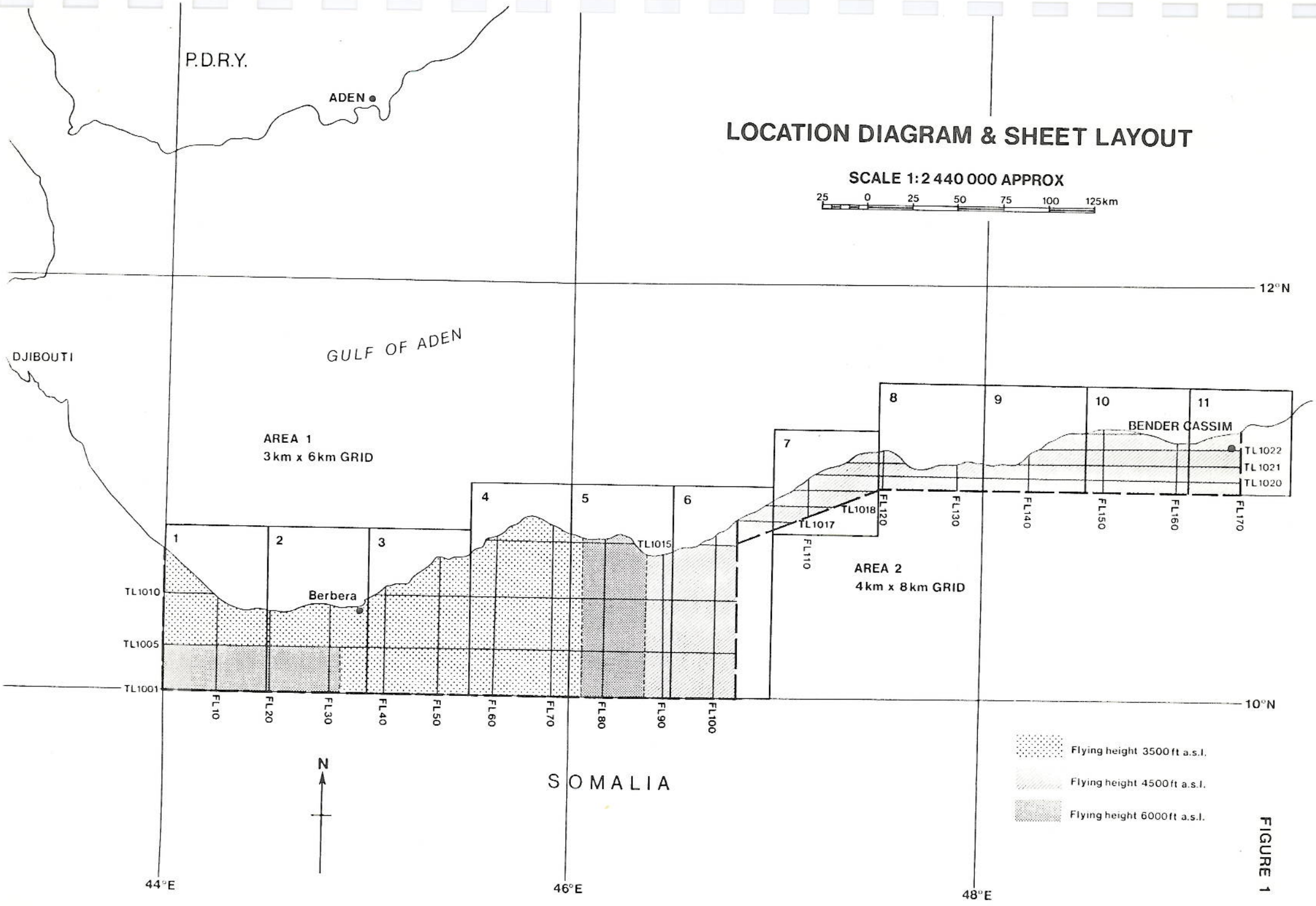
LOCATION DIAGRAM & SHEET LAYOUT
SCALE 1:2 440 000 APPROX
25 0 25 50 75 100 125km
P.D.R.Y.
ADEN
12°N
GULF OF ADEN
DJIBOUTI
AREA 1
3km x 6km GRID
AREA 2
4km x 8km GRID
1
2
3
4
5
6
7
8
9
10
11
BENDER CASSIM
TL1022
TL1021
TL1020
TL1018
TL1017
TL1015
TL1010
TL1005
TL1001
Berbera
FL10
FL20
FL30
FL40
FL50
FL60
FL70
FL80
FL90
FL100
FL110
FL120
FL130
FL140
FL150
FL160
FL170
N
SOMALIA
10°N
44°E
46°E
48°E
Flying height 3500ft a.s.l.
Flying height 4500ft a.s.l.
Flying height 6000ft a.s.l.

FIGURE 1

2. GEOLOGY

2.1 PHYSIOGRAPHY

The survey area extends for approximately 570 km along the coast of Northern Somalia between longitudes 44°E and 49°15'E, and from the coast to the foothills of the plateau to the south. In the east, the southern survey boundary is controlled by Jebel Warsangeli, (Figure 1).

2.2 GEOLOGICAL SUCCESSION

2.2.1 Basement

The Basement ranges in age from Pre-Cambrian to early Palaeozoic and is divisible into three major rock types:

(i) the younger Inda Ad metasedimentary series;

(ii) an older series of metamorphic gneisses and migmatites;

(iii) a unit composed of igneous rocks that range from acid to ultrabasic in composition.

The latter rocks are intruded into the other units of the Basement Complex.

2.2.2 Sedimentary Succession

This has been summarised by Z.R. Beydoun (1970) as follows:

Oligo-Miocene to Pliocene	includes Hafun Limestones
Mid-Eocene	Karkar Limestone
Lower to Mid-Eocene	Taleh/Gypsum-Anhydrite Series
	Transitional contact
Mid-Palaeocene to Lower-Eocene	Auradu Limestone
Cretaceous	Nubian Sandstone
	Gawan Limestone) not present Daghani Shale) east of 47°30'E.
Upper Jurassic	Wanderer Limestone
	Gahodleh Shale
	Bihen Limestone
Lower Jurassic	Adigrat Sandstone
	Major Unconformity
Pre-Cambrian - Early Palaeozoic	(Basement)

Between 46°07'E and 47°30'E the whole of the Jurassic section is missing and the Cretaceous lies directly on the basement.

The total thickness of sediments as recorded in boreholes is approximately 6 km.

2.3 IGNEOUS ACTIVITY

The only recorded intrusive or volcanic activity within the survey area are: intrusive rocks throughout the Basement Complex; a locally developed lava flow or minor basaltic intrusion at the base of the Adigrat in the Karin-Asseh Basin; and the dykes, sills and related extrusives of the Tertiary Aden Volcanic series, seen in the region surrounding the Bulhar Plain.

2.4 TECTONIC SETTING

The structural framework of the survey area is controlled by major faulting in three directions (Baker 1970):

(i) The Red Sea Trend. These are structures associated with the opening of the Red Sea, and orientated northwest - southeast to east - west e.g. in the Baqayeleh region.

(ii) The East African Rift Trend. These north - south features are thought to be associated with the East African Rift e.g. the fault east of Buuraha Gal Dhufaan.

(iii) The Gulf of Aden Trend. The opening of the Gulf of Aden is thought to have caused westnorthwest - eastsoutheast normal faults and dextral translation along northnortheast - southsouthwest faults seen cropping out in the Ardadle and Kabaleis mountains.

In addition to these tectonic trends, there are variations in orientation of basement structures from northeast-southwest to northwest - southeast which may further complicate the overall picture. Many of these are visible in the Shimberaleh Plain. For further details of the tectonic framework, the reader is directed to Laughton et al (1970) and Whitmarsh (1981).

2.5 SOURCES OF MAGNETIC ANOMALIES

Within the survey area there are three possible sources of magnetic anomalies caused by contrasts in magnetic susceptibility.

These contrasts can occur:

(i) between magnetic basement and the sedimentary section;

(ii) between basic or ultrabasic intrusives within the basement and either the overlying sedimentary section or, less frequently, magnetic basement itself;

(iii) between the Aden Volcanics and the sedimentary section.

2.6 HYDROCARBON POTENTIAL

Since the 1950's and earlier, active hydrocarbon exploration has taken place in the Horn of Africa after an oil seepage was reported in former British Somaliland. (Somaliland Oil Exploration Co. Ltd., 1954). This has resulted in several boreholes being drilled within the survey area. Subsequent exploration has been extended over much of the country and into offshore areas. In more recent years the increased knowledge regarding the evolution of hydrocarbons and their entrapment has sustained the search for oil-bearing rocks in what has to date been a relatively barren area.

3. PRESENTATION OF RESULTS

The results of the aeromagnetic survey are presented as follows:

(i) Eleven map sheets showing the aircraft's flight track with the coastline and concession boundary at 1:100,000 scale.

(ii) Eleven map sheets of total magnetic intensity contours, computer drawn at 1:100,000 scale, with flight track, coastline and concession boundary in subdued form.

(iii) Eleven sheets of magnetic interpretation at 1:100,000 scale showing magnetic basement isobaths and major magnetic features e.g. faults, intrusives, and intrabasement and intrasedimentary features. The flight tracks, coastline and concession boundary are shown in subdued form.

(iv) Two map sheets at 1:250,000 scale showing the aircraft flight track, and the coastline and concession boundary.

(v) Two map sheets of total magnetic intensity at 1:250,000 scale.

(vi) Two map sheets of magnetic interpretation at 1:250,000 scale.

(vii) Computer plotted CALCOMP profiles for all flight and tie lines at 1:100,000 horizontal scale showing the following data:

(a)	ground clearance	scale	50 m/cm
(b)	total intensity (ground)	scale	5 nT/cm
(c)	total intensity (air)	scales and	5 nT/cm 25 nT/cm
(d)	horizontal gradient	scale	0.1 nT/sec/cm

(viii) A magnetic archive tape of all relevant aeromagnetic and navigation data. Its format is given in Appendix A of the Operations Report.

4. INTERPRETATION METHODS

4.1 INTRODUCTION

The interpretation is based on an analysis of the total intensity contour maps at 1:100,000 scale and of the CALCOMP profiles.

The interpretation comprised the following stages:

(i) An examination of all flight line CALCOMP profiles, during which anomalies were analysed and depths estimated using the methods described in Section 4.3. The depth estimates were plotted on copies of the 1:100,000 flight track maps. As the horizontal gradient profiles were plotted as CALCOMPS for all lines, they were very useful in rapidly locating inflection points, measuring slopes, and locating points of half and three-quarter maximum slope. Their use speeded up the interpretation and considerably improved the accuracy of the derived results.

(ii) On examination of the contour maps, those depth estimates plotted in Stage (i) that were now seen to be unsuitably related to overall anomaly patterns were examined further but not eliminated. In addition, selected anomaly groups were recognised as being suitable for further analysis by interactive computer modelling.

(iii) A further examination of the contour maps enabled recognition of zones of differing magnetic character within the survey area. Major trends and discontinuities within these trends were identified.

(iv) After correction for obliquity and for the aircraft's flying height, the results of the above steps were compiled onto the interpretation worksheets. Those depth values attributed to magnetic basement were contoured, and any remaining inconsistencies were examined and resolved. In particular the presence of shallow-source anomalies in areas of deeper basement had to be studied.

4.2 MODEL ANOMALIES

The geomagnetic field values in the survey area are:

Inclination	+7° North
Declination	0°20'E
Total Magnetic Intensity	37000 nT

Magnetic intensities are expressed in nanoTeslas (nT), the SI unit, (1 nanoTesla = 10^{-9} Weber metres $^{-2}$) and is numerically equivalent to the gamma (1 gamma = 10^{-5} Oersted).

In calculating each depth estimate from observed magnetic anomalies a hypothetical model must be selected and assumed to approximate the geological feature causing the observed anomaly. Two basic models were assumed for this interpretation; these models, illustrated in Text Figure 2, all have vertical sides and horizontal faces only, and are the bottomless prism and the step or fault. However, occasionally a 3 - dimensional model may be more applicable to bodies of limited lateral extent.

Text Figure 2 shows computed anomalies over some of these models at strikes of 0°, 90° and 135°, inductively magnetised only, and at a magnetic inclination of +7° and a total intensity of 37000 nT. Also shown are the prism of limited vertical extent (or plate) and the vertical dyke. Their major characteristics are noted below:

(a) Vertical bottomless prisms exhibit a strong negative anomaly which is flanked on the equatorial side by a very weak positive anomaly.

(b) Steps or faults in which more-magnetic rocks are deeper to the south, exhibit a predominantly positive anomaly flanked to the north by a weaker negative. Steps or faults, in which the more-magnetic rocks are deeper to the north, exhibit a predominantly negative anomaly flanked to the north by a weaker positive. These faults are characterised by the negative component of the anomaly occurring over the upthrown side.

(c) Prisms of limited vertical extent (plates) have anomalies generally similar to those of great vertical extent, but a flanking positive anomaly occurs to both north and south of the main negative, that to the south being of greater amplitude than in case (a) above.

However, it will be noted from Figure 2 that as the strike of these models approaches 0°, their anomalies undergo a very significant change in both shape and polarity; and that in some models, the response is effectively zero.

4.3 QUANTITATIVE INTERPRETATION

4.3.1 Approximate Methods

Straight Slope Method. In this method the horizontal length of the straight part of the anomaly's steepest flank is used as a depth index. For anomalies of amplitude greater than a few tens of nanoTeslas, and where the straight slope occupies about half the total anomaly amplitude, the straight slope length is divided by unity; the model assumed in this case is the bottomless prism (Vacquier et al, 1951).

Generally, the results from this method are only a first approximation of the depth to the body; and unless estimates by other methods (which may be used if the anomaly is well defined) confirm the results of this method, they must be used with considerable caution.

Peters' Half-Slope Method. This method (Peters, 1949) uses the horizontal distance between the points on each side of an inflection at which the slope of the anomaly curve is one half of the maximum slope (i.e. that at the point of inflection). This horizontal distance is proportional to the depth of burial, and so is divided by a constant (usually between 1.8 and 2.0 for broad bodies) to give an estimate of depth to the upper surface.

4.3.2 More Accurate Methods

Bean's Method. The method due to Bean (1966) uses both limbs of an anomaly and yields measurements of inclination of magnetisation, susceptibility and depth. It is accurate, rapid to use and can also be used on incomplete anomalies.

50 - 75 Method. This method uses the half and three-quarter slopes in much the same way as Bean's method to gain a depth estimate.

Peter's, Bean's and the 50-75 method are made easier and quicker to use by having the computed horizontal gradient profiles presented on the CALCOMPS.

All the above methods assume the bodies are two-dimensional (i.e. the anomaly length is greater than five times the width). Three-dimensional anomalies were generally interpreted by the straight slope method applied to several limbs.

All the depth estimates have been related to sea level, being negative below sea level and positive above.

4.3.3 Computer Modelling

Computer modelling was carried out interactively to confirm the hypothesis that at this low magnetic latitude, positive anomalies can generally be assumed to indicate the shape of magnetic basement troughs and vice-versa, if there is no lateral change in basement susceptibility. Modelling also confirmed the agreement between the limited amount of gravity data available and the interpretation of the magnetic data. In all, five magnetic profiles were modelled, and Figures 3 to 7 show the observed and computed results across the three basins that were traversed by the profiles. The results of this modelling and inferences drawn are discussed fully in Section 5.3.

MAGNETIC MODEL ANOMALIES AT INCLINATION 7°

T = 37000 nT

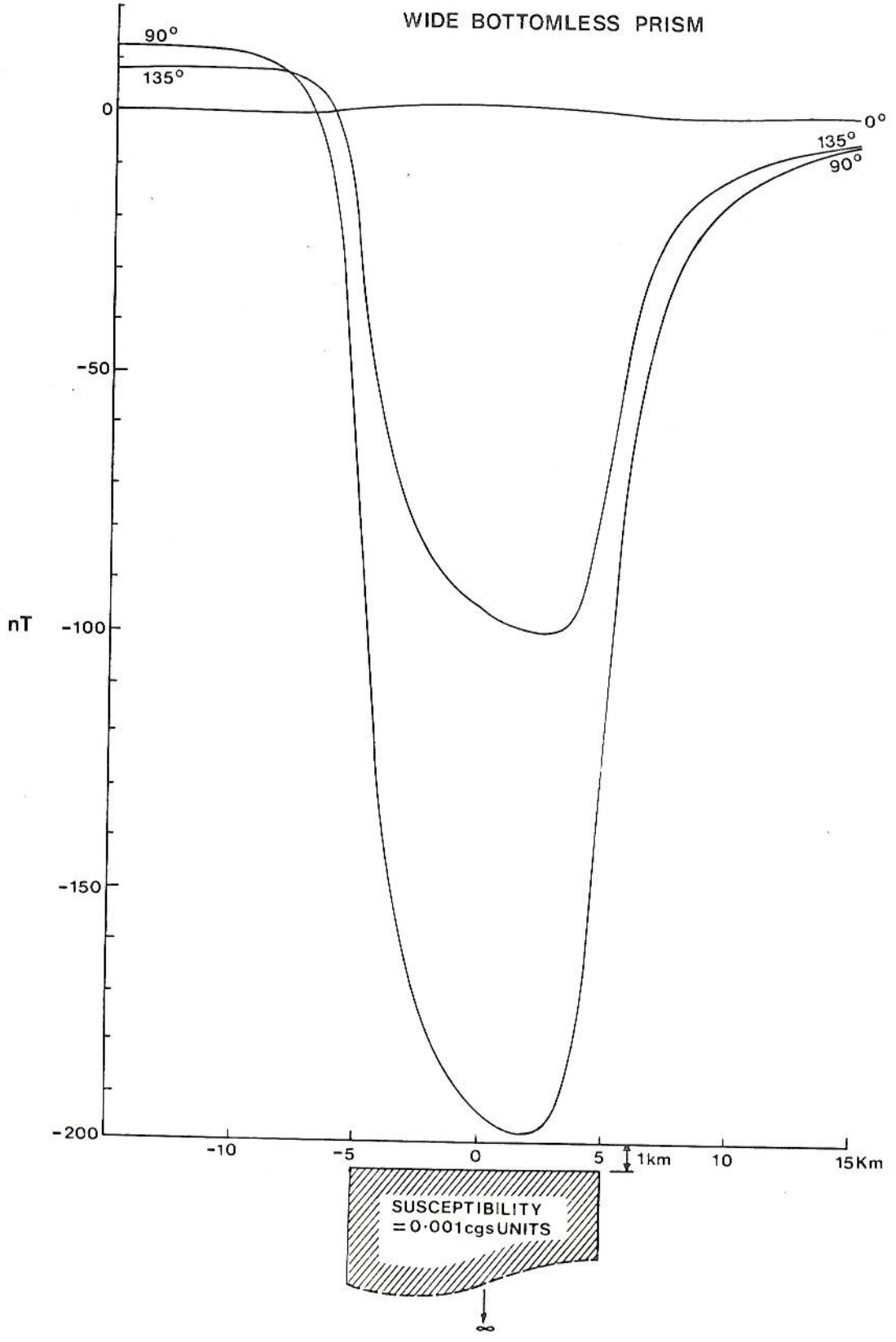

MAGNETIC MODEL ANOMALIES AT INCLINATION 7°

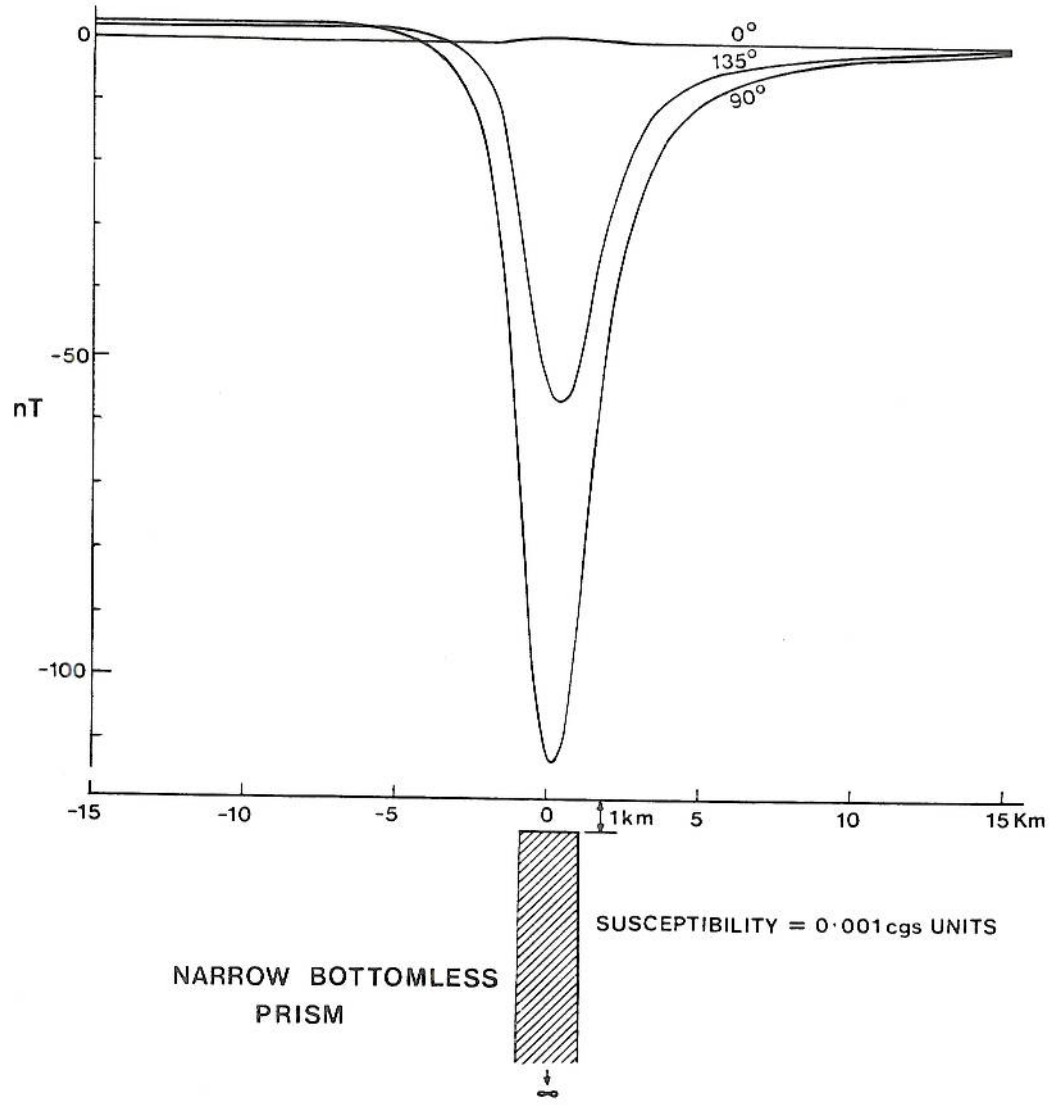

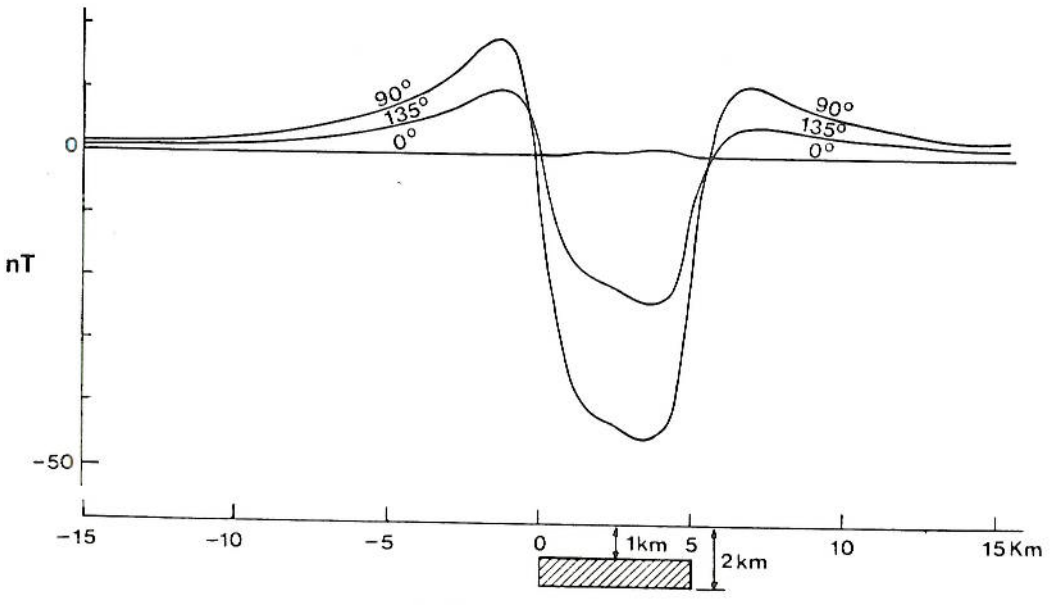

SUSCEPTIBILITY = 0·001 cgs UNITS

PLATE

MAGNETIC MODEL ANOMALIES AT INCLINATION 7°

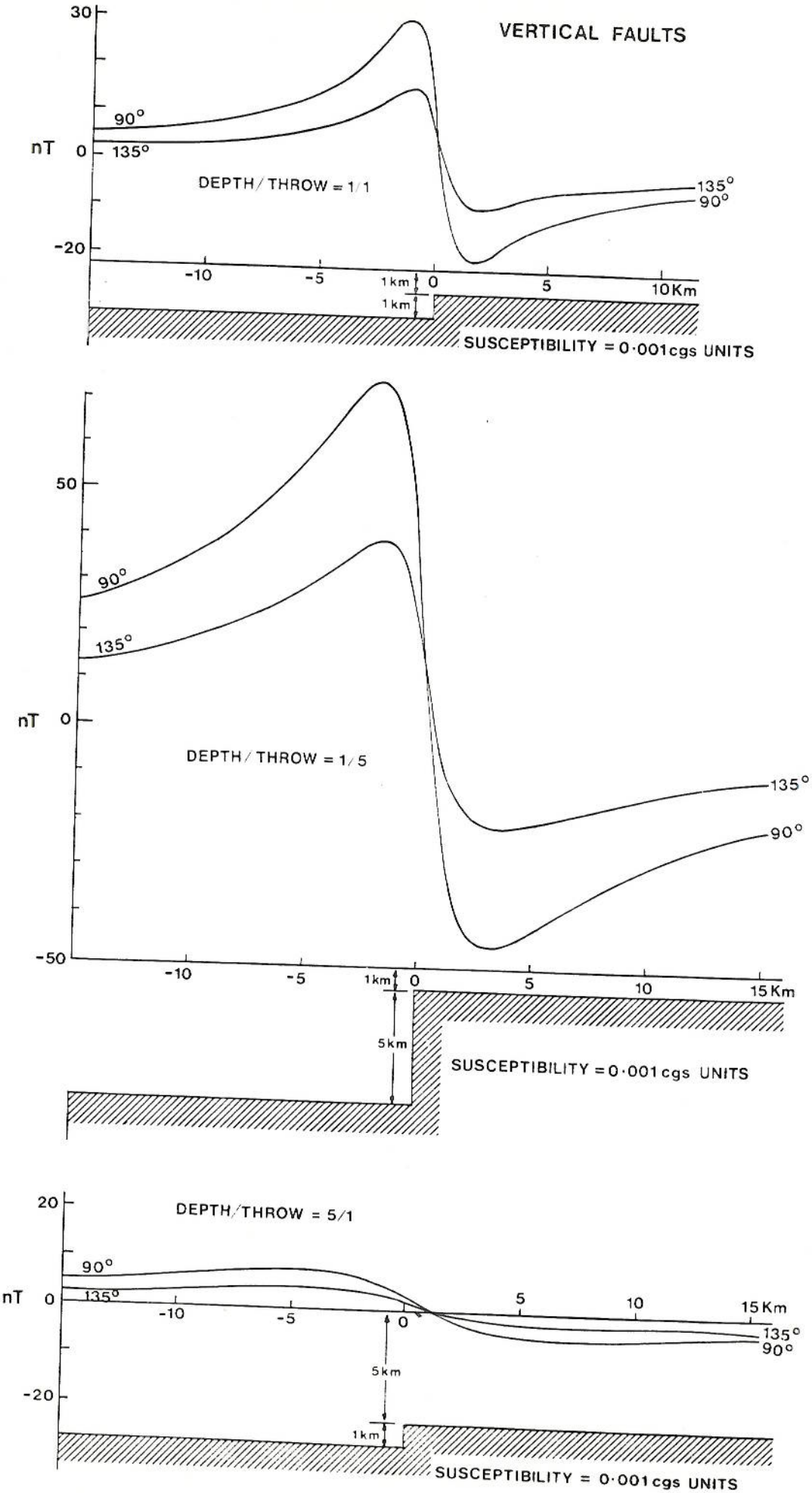

5. DESCRIPTION OF DATA AND INTERPRETATION

5.1 THE MAGNETIC CONTOUR MAPS

The total intensity contour maps exhibit four zones divisible on the basis of character, distribution and intensity of the anomalies.

(i) An area of broad, well-defined anomalies interspersed with narrow, high-amplitude anomalies (over 150 nT) with 20 - 30 km east-west strike length. These cover Sheets 1, 2, and 3 and the northeast of Sheet 4.

(ii) To the east of zone (i) is an area of low magnetic relief and no strong trend except in the extreme south where an east-west feature is clearly visible. This area covers the remainder of Sheet 4 and most of Sheet 5.

(iii) The southeast of Sheet 5, Sheet 6 and most of Sheet 7 are characterised by fairly short-wavelength anomalies of 50 - 150 nT amplitude with a long strike length and pronounced orientation similar to the high-amplitude anomalies present in zone (i). The main trend of the anomalies is west northwest - east southeast over the northern part of the area with a more east - west trend gaining predominance in the south of Sheets 5 and 6.

(iv) In the east on Sheets 8 to 11 the magnetic contours show a gradient generally striking east - west which may be related to topographic relief. Superimposed on this are a few east - west orientated, low-amplitude anomalies of less than 50 nT.

5.2 INTERPRETATION MAPS

5.2.1 General

The interpretation maps contain the following information:

(i) Depth estimates from three types of magnetic structure. These are:

(a) Intrabasement estimates, which have been interpreted as having their source below the magnetic basement surface. These can be seen, for example, on Sheets 3 and 8.

(b) Depth estimates considered to be due to features on the upper surface of magnetic basement; it is on these estimates that the basement contours have been compiled.

(c) Depth estimates of magnetic features lying above magnetic basement i.e. within the sedimentary section. These occur mainly on Sheets 1 and 5.

(ii) Basement depth contours (isobaths) showing the interpreted basement surface with respect to sea level. The contours are at 0.5 km intervals. Twelve basement high axes and twenty basement low axes are marked and referenced by H1-H12 and L1-L20. The principal axes are listed in Table 1 along with their locations and depth limits.

(iii) Twenty one major faults are interpreted from the basement features and are identified by F1-F21.

(iv) Eight intrusions have been outlined. As all eight are considered to be part of the magnetic basement, all depth estimates related to these intrusions have been contoured as forming part of the upper surface of the basement.

5.2.2 Basement Structures

The basement structures can be categorised into four main zones on the basis of structural direction and grain. These zones are separated by faults F11-F12, F20, and basement low axes L17.

(i) Zone 1

Zone 1 extends across the western part of the area as far as F11 and the northern continuation of F12. It covers all of Sheets 1 - 3 and part of 4. This zone is dominated by three major low axes trending east - west to west northwest - east southeast (L2-L4) and which form a semi-continuous basin across the whole zone, some 180 km long, reaching a maximum depth of - 6.9 km in the east and - 4.0 km in the west. In the west of this zone faults F1-F3 divide this structure from basement high H1 that includes, in part, a feature which has been interpreted as an ultrabasic intrusion within the basement. To the north of H1 is a small basin L1 which is incompletely defined and only based on a few depth estimates, reaching a maximum depth of - 2.5 km within the survey area. Ultrabasic intrusives on Sheet 3 between L4 and L5, and are partially fault controlled by F5-F9 inclusive.

As L5 is based on the magnetic TI pattern and only a single depth estimate, it should not be regarded as a definite structure.

On Sheet 3, L4 shows strong control by faults. It is bounded to the south by series of faults (F5 to F9) and is divided from H2 in the north by another fault (F10).

To the north of H2 and H3 are two basins (L6 and L7) showing a more northeasterly trend than seen in the rest of Zone 1. Though this is similar to the orientation of F10, the basement contours in this region should be treated with caution due to the absence of accurate depth estimates.

Low L9 lies between F11 and F12 and has a north - south orientation. This is thought to be related to the East African Rift Valley Trend because of its orientation.

(ii) Zone 2

Zone 2 lies between faults F12 and F20 on Sheets 4 and 5 and shows no single dominant orientation. Here the basement structures are possibly controlled by the interaction of the Rift Valley Trend shown in L8, L12 and H6 and the Red Sea, or possibly, Gulf of Aden Trends which are shown by L10, L11, H5 and H7. Basin L10, which is the largest in this zone, reaches a maximum depth of - 4.0 km.

Faults F13, F15 and F16 strike east - west (Red Sea Trend) and are offset by F14 which may be, due to its orientation, associated with the Rift Valley Trend.

(iii) Zone 3

This zone extends from F20 eastwards to L17; it is characterised by parallel to sub-parallel ridges and troughs ranging from 15 to 60 km long. In the north of this zone the trend of these structures is west northwest - east southeast to northwest - southeast shown by L17, L16 and H8. In the southern part of this zone however, the dominant trend is east - west as shown by F18, F19, L13 and H10. Between H10 and H8 both above trends are apparent and the structural framework is made up of short some-

times interconnecting ridges and troughs with parts of some features exhibiting one trend and other parts of the same feature showing the other trend e.g. H9, L14 and L15. The maximum depth to basement in this zone is - 2.3 km in L14.

F21 and F20 both appear to be related to the Rift Valley Trend.

(vi) Zone 4

Zone 4 extends eastwards from L17 due to the shape of the survey area. In this region many of the features seen are incompletely defined, so this and the wide distribution of depth estimates have led to large sections of contours being interpolated along total intensity features, consequently there is a loss of definition of basement structure in this region.

In the west of this zone (Sheets 7, 8, 9) most structures show an east - west general trend (H11, H12) becoming slightly more east northeast - west southwest towards the centre of this zone (L18, H12?). The eastward continuation of L18, i.e. L19, trends more northeast - southwest but the contours, and therefore the axis, are only based on a few widely spaced depth estimates, so this apparent change in direction may not in fact, exist.

L20 in the extreme east of this region is incompletely defined but its apparent trend is northwest - southeast and it reaches a maximum depth of - 3.6 km.

TABLE 1 LIST OF MAJOR BASEMENT STRUCTURES

Basement Low	Max. Depth (km)	Sheet No.	Basement High	Min. Depth (km)	Sheet No.
L1	- 2.5	1	H1	0.2	1
L2	- 5.0 approx.	1	H2	- 0.1	3
L3	- 4.0 approx.	1 - 2	H3	- 0.5	3 - 4
L4	- 6.9	3	H4	0.5	4
L5	- 0.5 approx.	3	H5	0.0	4
L6	- 1.5 approx.	3	H6	0.5	5
L7	- 5.5	3 - 4	H7	0.1	5
L8	- 3.9	4	H8	0.5	5 - 6
L9	- 3.3	4	H9	0.5	5 - 6
L10	- 4.0	4 - 5	H10	0.4	5 - 6
L11	- 2.3	4 - 5	H11	- 0.4	7 - 8
L12	- 3.4	5	H12	0.8	8 - 9
L13	- 1.5	5			
L14	- 2.3	5 - 6			
L15	- 2.3	5 - 6			
L16	- 0.7	5 - 6			
L17	- 2.5	7 - 8			
L18	- 2.9	8 - 9			
L19	- 2.5	9 - 10			
L20	- 3.6	11			

5.2.3 Faulting

Several inferred faults have been shown on the interpretation map as marking boundaries between zones of differing magnetic character e.g. F12 and F20 or where basement depth estimates and/or total intensity gradients indicate a sharp change in basement depth i.e. F1, F2, F13 - 18, for example.

Other basement gradients not specifically marked as faults on the interpretation map may be faulted e.g., the gradient between the western edge of H7 and L8 on Sheets 4 and 5, or H6 and L12 on Sheet 5, or H9 and L14 on Sheet 6.

Another possible fault could be a northward extension of F12 (on Sheet 4) along the break in basement slope to the west of L8. F12 on Sheet 6 could also be extended to the south.

5.3 COMPUTER MODELLED PROFILES

A total of five magnetic profiles were modelled across three major basement structures. All the models assumed 2-dimensional bodies and no remanent magnetisation. Attempts were also made to minimise lateral changes in basement susceptibility whenever possible so as to produce as general a solution as possible.

(i) Profiles AA and BB were run across L3 and H1 on Sheet 1. Both computed models show similar features with a vertical step (F4) to the south of the basin (L3) and an increase in magnetic susceptibility northwards. The maximum basin depth is in excess of 4 km on AA and is marginally shallower on BB.

(ii) Profiles CC and DD were constructed across L4 and H2 - 3 on Sheet 3. They both show the major basin underlain by magnetic basement of uniform susceptibility to the south separated from the basin by faults F7 and F9 respectively.

(iii) Profile EE was run across H9, H10 and L14/L15; the model used was directly based on the interpreted basement contour intercepts thus confirming the interpreted basement structure within the limitations of the modelling procedures.

To summarise, the computed models confirmed that the interpreted basement structures are consistent with the observed total intensity data.

5.4 COMPARISONS WITH OTHER AVAILABLE DATA

The correlation between outcropping ultrabasic intrusions, e.g. on Sheet 3, and intense magnetic lows was used to infer the existence of similar buried intrusives on Sheet 1 and in other parts of Sheet 2 and 3. Other than the marked intrusive on Sheet 6 of the interpretation, other intrusives may be present, especially within H9 and possibly within the smaller high axis to the south of H9. These possible intrusives have not been outlined due to their slightly lower magnetic response and weaker surrounding gradients, which could be due to rocks other than ultrabasics within the basement.

An area of outcropping basement on Sheet 5 was not defined by the magnetic data and it must therefore be assumed to have a low or non-existent magnetic susceptibility contrast with the surrounding rocks.

COMPUTED MAGNETIC PROFILE ACROSS SECTION AA

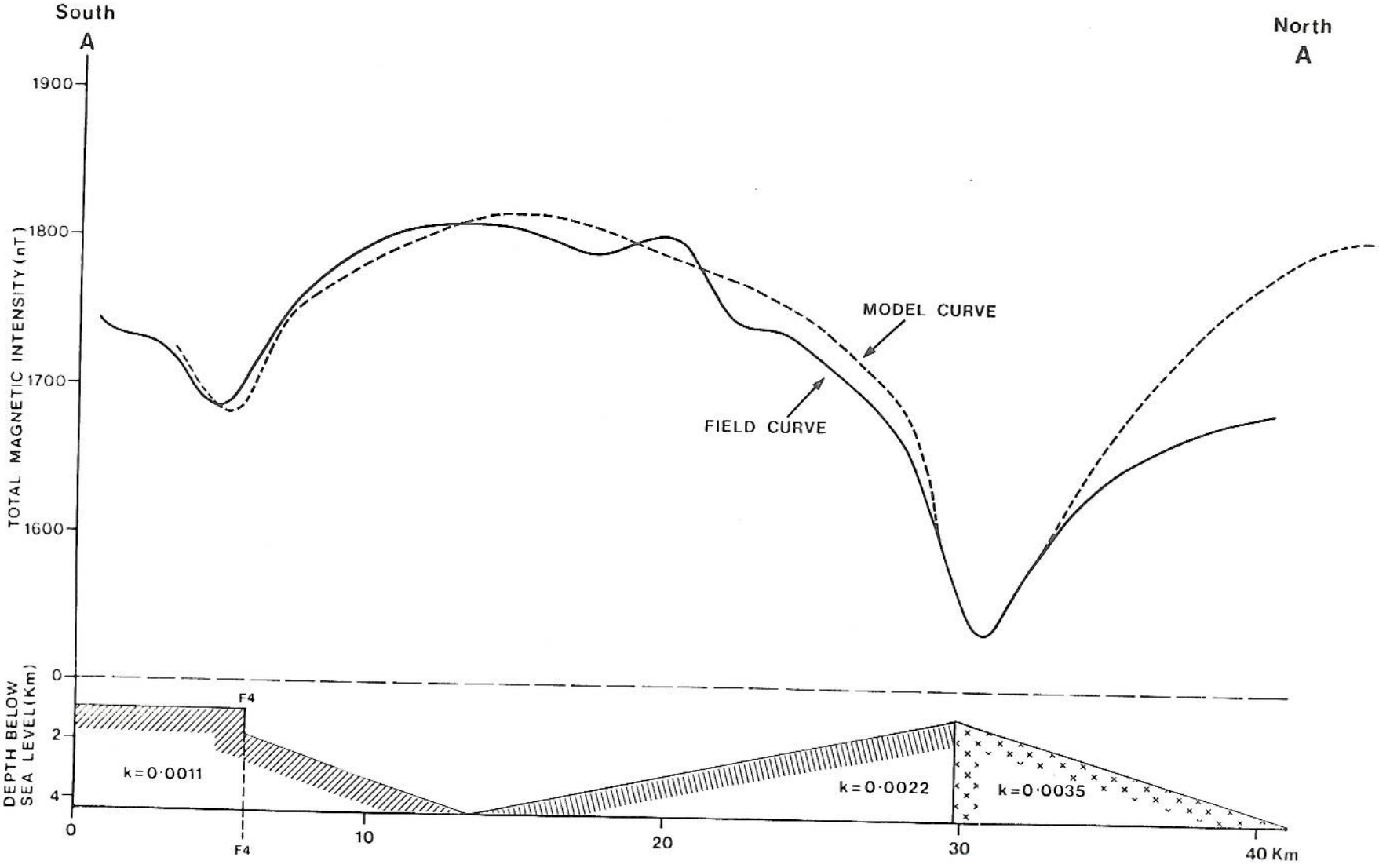

SCALE 1:200 000

FIGURE 3

COMPUTED MAGNETIC PROFILE ACROSS SECTION BB

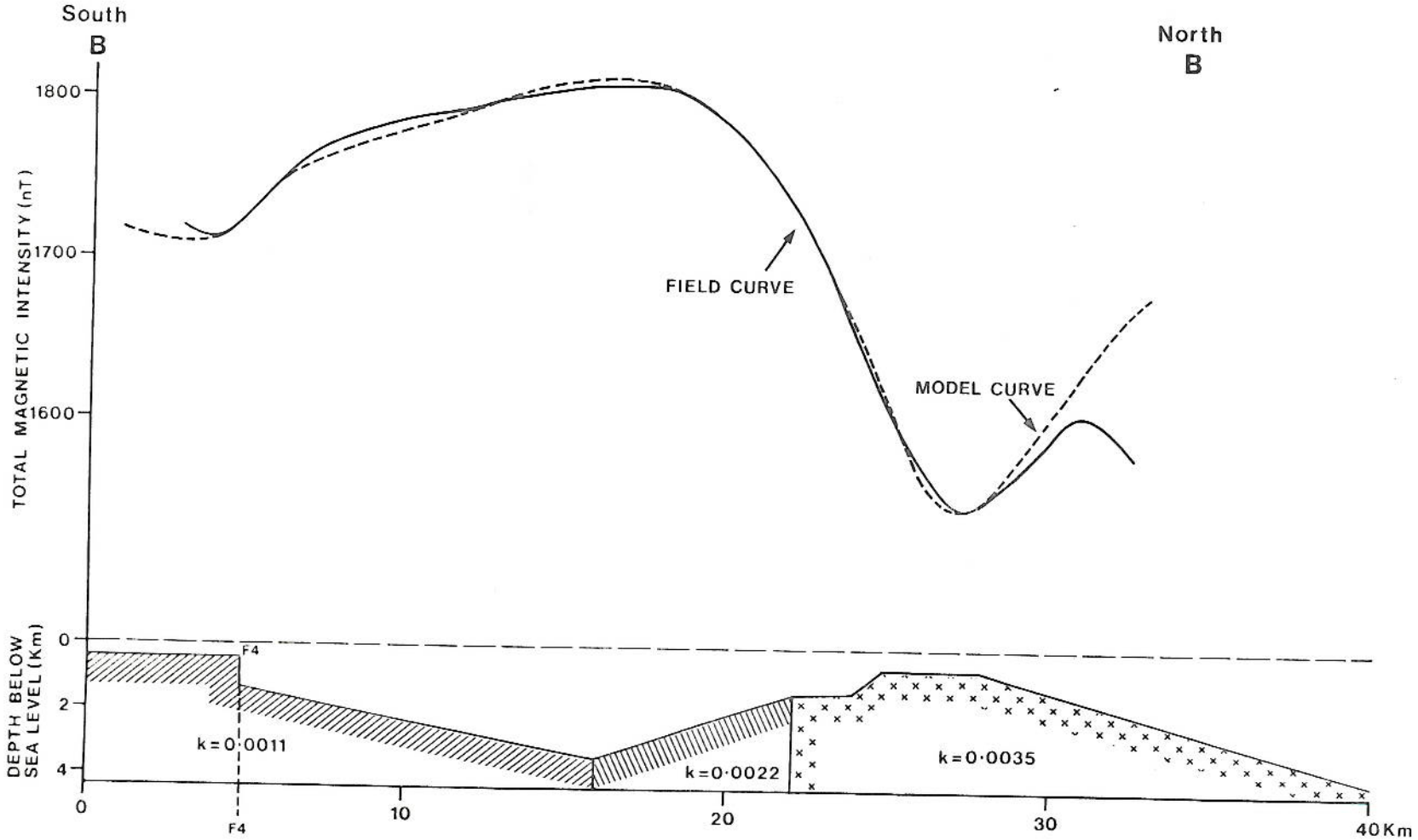

SCALE 1:200 000

FIGURE 4

COMPUTED MAGNETIC PROFILE ACROSS SECTION CC

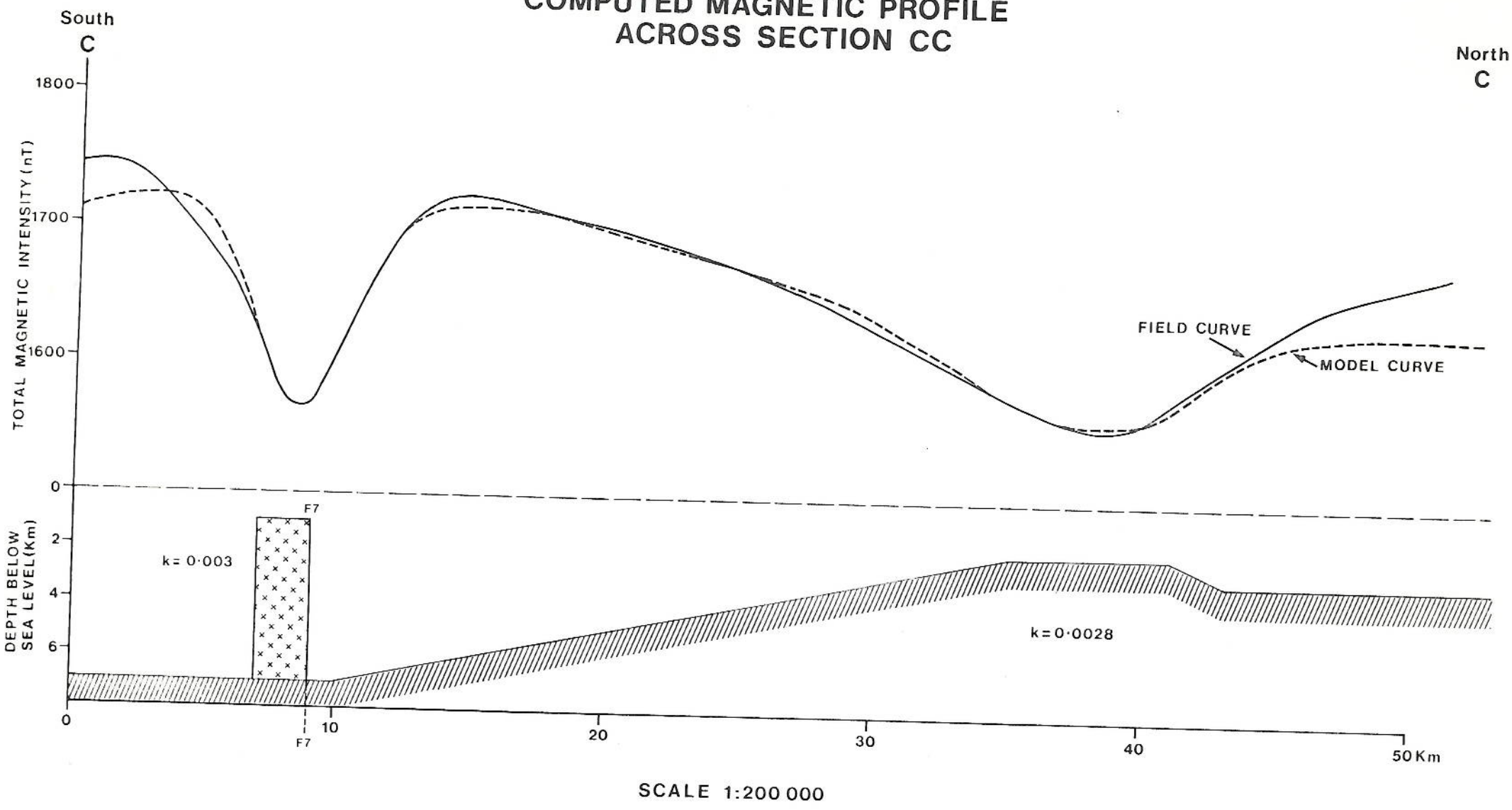

SCALE 1:200 000

FIGURE 5

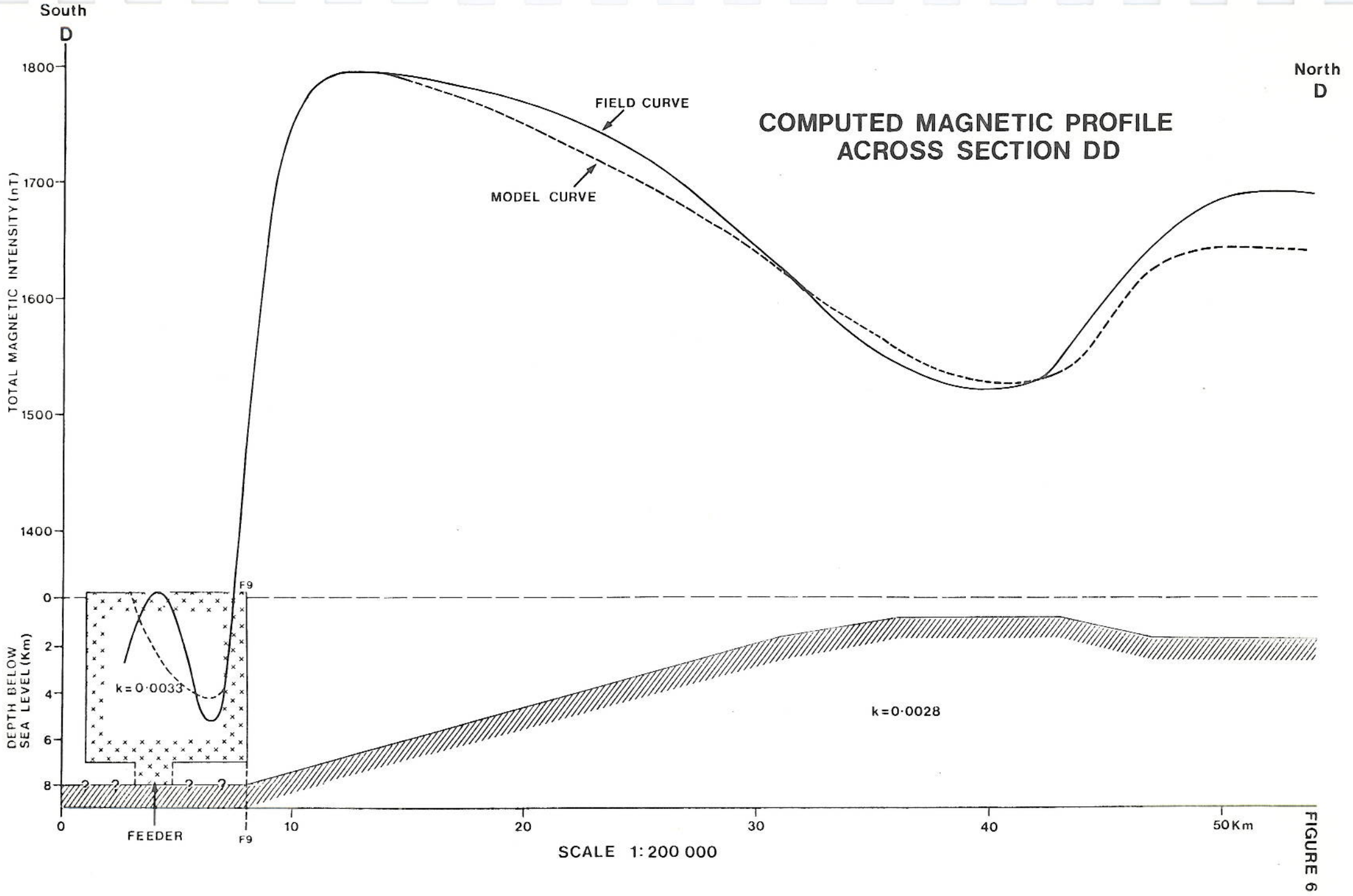
South
D
North
D
COMPUTED MAGNETIC PROFILE
ACROSS SECTION DD
FIELD CURVE
MODEL CURVE
TOTAL MAGNETIC INTENSITY (nT)
1800
1700
1600
1500
1400
DEPTH BELOW SEA LEVEL (Km)
0
2
4
6
8
F9
k = 0·0033
k = 0·0028
? ? ? ? ?
FEEDER
F9
0
10
20
30
40
50 Km
SCALE 1: 200 000
FIGURE 6

COMPUTED MAGNETIC PROFILE
ACROSS SECTION EE

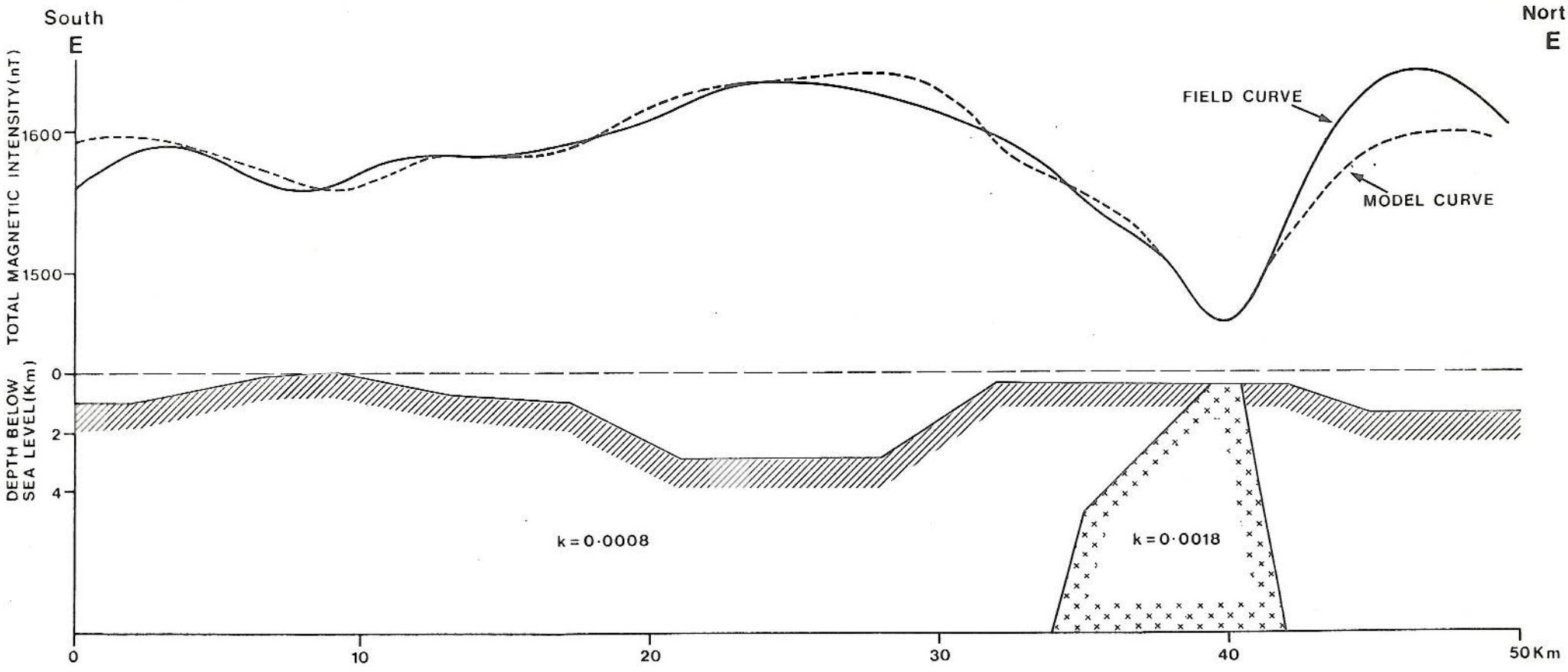

SCALE 1:200 000

FIGURE 7

A number of small basins have been photogeologically mapped in the south of Sheets 1 and 2 and in the southwest of Sheet 3 .They occur within areas of mainly outcropping basement. It has not proved possible to define these basins from the results of this survey due to the lack of resolution of the magnetic method.

Anomalies due to the Aden Volcanics on Sheet 1 are not as widespread or as strong as would be inferred from the surface geology. Therefore either the volcanics are of limited depth extent, or the volcanics have been heavily weathered and the magnetic minerals within them have been oxidised to haematite which is weakly magnetic.

A limited amount of gravity data were available over parts of Sheets 3 and 4. These data confirmed the interpreted magnetic basement structure. The single gravity traverse across L4 (on Sheet 3) yielded a maximum possible depth to basement of approximately 7 km below sea level using Smiths formulae (Smith 1960).

6. RECOMMENDATIONS

Due to the lack of clear inflection points and hence depth estimates in certain areas, specifically around L3, L4 and L20 on Sheets 1, 3 and 11 respectively, it is recommended that gravity profiles be acquired to confirm and possibly refine these structures.

The structural pattern within Zone 2 of the interpretation on Sheets 4 and 5 may be more clearly resolved with the acquisition of gravity data to confirm the dimensions, and the inter-relationship of lows L8, L10 and L12. However, it should be pointed out that gravity and magnetic surveys respond to different physical parameters and therefore the interpretations may not necessarily coincide exactly, but could parallel each other, the 'gravity basement' more likely being shallower than 'magnetic basement'.

7. ACKNOWLEDGEMENTS

We acknowledge the assistance of James Moffat and Graham Hurd and the provision of borehole and geological data by the staff of Quintana Somalia Limited.

BIBLIOGRAPHY

Baker, B. H.	1970	The structural pattern of the Afro-Arabian Rift system in relation to plate tectonics. Phil. Trans. Roy. Soc. Lond. A, 267, 383-391
Bean, R. J.	1966	A rapid graphical solution for the aeromagnetic anomaly of the 2 - dimensional tabular body. Geophysics 31(5), 963-970
Beydoun, Z. R.	1970	Southern Arabia and northern Somalia: comparative geology. Phil. Trans. Roy. Soc. Lond. A, 267, 267-292
IAGA Division 1 Study Group	1976	International Geomagnetic Reference Field 1975. EOS Transactions, AGU, 57, 120-121
Laughton, A. S., Whitmarsh, R. B., Jones, M. T.	1970	The evolution of the Gulf of Aden. Phil. Trans. Roy. Soc. Lond. A, 267, 227-266
Peters, L. J.	1949	The direct approach to magnetic interpretation and its practical applications. Geophysics 14(3) 290-320
Smith, R. A.	1959	Some depth formulae for local magnetic and gravity anomalies. Geophys. Prosp. 7,55-63
Somaliland Oil Exploration Co. Ltd.,	1954	A geological reconnaissance of the sedimentary deposits of the Protectorate of British Somaliland. Crown Agents for the Colonies, 42p p
Vacquier, V., Steenland, N.C., Henderson, R. D., Zeitz, I.	1951	Interpretation of Aeromagnetic Maps Geol. Soc. Am. Memoir 47
Whitmarsh, R. B.	1981	Geophysical Controversy in the Gulf of Aden. Nature, 291, p 375-376

PART 2

OPERATIONS REPORT

1. INTRODUCTION

The aeromagnetic survey described in this report was carried out by Hunting Geology and Geophysics Limited on behalf of Quintana, Somalia Ltd. The survey contained a total of 14,419 line kilometres of which 14,379 line kilometres was used for compilation. The survey area is shown in Figure 1. Flying commenced on 14th July, 1981 and was completed on 13th November, 1981, the crew being stood-down from 12th August to 1st October due to weather problems.

The aircraft used was a 'wet-lease' Douglas DC-3 supplied by Kenting Earth Sciences Ltd. of Ottawa, Canada. It was fitted with a CENG high sensitivity magnetometer, digital and analogue recorders, radar and barometric altimeters and a doppler navigation system.

The following sections describe field operations and data compilation procedures carried out for this survey.

2. PERSONNEL

The survey team supplied by Hunting was as follows:-

R. Stockham	Project Manager/Electronics Engineer
A.J. Billings	Geophysicist (Part-time)
G.D. Knight	Data Compiler (Part-time)
G.J. Osborn	Data Compiler (Part-time)
J. Danter	Data Compiler
J. Cook	Logistics Officer

Kenting provided the following aircrew:-

G.W. Carter	Aircraft Captain
B.T. Berrigan	Aircraft Captain
M.G. Kennedy	Pilot/Navigator
J.D. Pile	Pilot/Navigator
T. Urkosky	Engineer

3. FLYING OPERATIONS

3.1 AIRCRAFT AND OPERATIONAL BASE

The survey was flown using a DC-3, registration number C-GOZA, based at Hargeisa. Entry into and exit from Somalia for this aircraft was through Mogadiscio and Djibouti respectively.

3.2 FLYING SPECIFICATIONS AND TOLERANCES

The nominal flying specifications were as follows:

Flight line direction	North - south
Flight line spacing	3 km west of 46°50'E, 4 km east of 46°50'E
Tie line direction	East - west
Tie line spacing	6 km west of 46°50'E, 8 km east of 46°50'E
Line spacing tolerance	Not to exceed 6 and 8 km separation over a distance of 8 km or more.
Flying height tolerance	Not to exceed ± 70 feet.

Over the coastal plains the majority of the flying was at a height of 3,500 ft above sea level, but this had to be raised to 4,500 ft east of approximately 46°30'E to accommodate for the generally steeper slopes of Jebel Warsangeli and the surrounding mountain ranges. In the south of the area to the west of 45°E the flying height was raised to 6,000 ft in order to clear mountain peaks which attain 4,000 - 4,700 ft in this region. Between 46°E and 46°30'E the flying height was elevated to 6,000 ft to clear the Guveneh Mountains which rise to 5,400 ft.

3.3 NAVIGATION

Navigation was primarily visual, based on the 1:100,000 series topographic maps. Prior to the start of flying operations, these maps were mosaiced together, the flight lines marked onto them, and they were cut into strips suitable for handling in the aircraft cockpit.

As an aid to navigation, a Decca AD560 doppler navigation system was installed onboard the aircraft. This equipment enabled the pilot to fly the most accurate heading along each survey line.

3.4 SURVEY TIMING AND PROGRESS

The following is a diary of events:

8/7/81	Aircraft arrived Mogadiscio
12/7/81	Aircraft transit to Hargeisa
17/7/81	Air tests
24/7/81	First productive sortie
12/8/81	Standdown due to turbulence
1/10/81	Aircraft returned to Hargeisa
13/11/81	Last productive sortie
24/11/81	Aircraft demobilised to Djibouti

4. EQUIPMENT

4.1 MAGNETOMETERS

4.1.1 Airborne Magnetometer

This was an instrument based on the Overhauser Effect designed and built by CEA-CENG (Commissariat à l'Energie Atomique-Centre d'Etudes Nucléaires de Grenoble, France) and called Model MPPE 101. This equipment has a basic sensitivity of 0.01 nT.

The sensor head and preamplifier were installed in a bird towed 60 m under the aircraft. It gave a continuous output which was recorded in both analogue and digital forms.

4.1.2 Ground (storm) Magnetometer

This was a CENG magnetometer similar to the airborne instrument. The output was displayed on an analogue recorder and recorded digitally every five seconds.

This equipment showed that variations in the earth's diurnal field outside the specification occurred over a total of ten days during the survey, though some days production were also affected in part by excess diurnal variation.

4.2 DATA ACQUISITION AND RECORDING

4.2.1 Data Acquisition System

A GeoMetrics G714 data acquisition system was used to synchronise all recorder fiducial pens, fire the tracking camera, convert analogue data to digital and block up the resulting information into a format suitable for digital recording.

The G714 contains a stable quartz clock which is zeroed at the start of each day's flying; this tallies with the veeder counter mounted in the tracking camera and is automatically copied onto the tracking camera film.

4.2.2 Analogue Recorders

Two Hewlett Packard twin channel pen recorders were installed onboard the aircraft to display the output from the magnetometer, radar and barometric altimeters and doppler navigation system as well as time fiducials. Full scale deflections (FSD's) and chart speeds were as follows:

(i) HP 7100B, 10 inch chart width, speed nominally 1.2 ins/min.

- (a) Magnetometer trace, red pen; 10 nT per inch over 8 or 10 inches.
- (b) Radar altimeter trace, blue pen, 0-5,000 feet FSD.
- (c) Time fiducials (blue) every 10 seconds along the left hand chart margin. Doppler distance gone fiducials (red) every 1 km along the right hand chart margin.

(ii) HP 7132A, 25 cm chart width, speed doppler controlled to give true horizontal scale of 1:100,000.

- (a) Barometric altimeter trace blue pen, 100-0-100 feet over 20 cm (1 cm = 10 feet).

(b) Doppler across track output red pen, 12.5-0-12.5 km over 25 cm (1 cm = 1 km).

(c) Time fiducials (blue) every 10 seconds along the left hand chart margin. Doppler distance gone fiducials (red) every 1 km along the right hand chart margin.

The ground magnetometer output was displayed by a single channel 10 cm chart recorder; the speed was 0.8 cm/min approximately and the chart scale 1 nT/cm giving 10 nT FSD for most of the survey. From the 22nd November, 1981 the chart scale was reset to 40 nT FSD.

4.3.2 Digital Recorders

The information from the G714 data acquisition system was recorded in blocks of ten records by a Kennedy digital tape recorder. The data formats are given in Appendix A.

The ground magnetometer contained a digital cassette recorder as an integral part of the equipment.

4.3 ANCILLARY EQUIPMENT

4.3.1 Altimeters

The aircraft carried a TRT AHV8 radar altimeter to record the actual ground clearance; a Rosemount barometric altimeter enabled the pilot to maintain the specified barometric flying heights. Both altimeter outputs were recorded in analogue and digital forms.

4.3.2 Tracking Camera

The aircraft's flight track was recorded using a Vinten Mk II 35 mm half-frame tracking camera with a wide angle lens. It was mounted vertically in the body of the aircraft. The camera was triggered every two seconds by the G714 data acquisition system and each frame displayed a time fiducial number corresponding to that of the G714 master clock. The firing interval enabled adequate forward overlap between successive frames to ensure continuous coverage of the flight tracks.

4.4 DOPPLER NAVIGATION SYSTEM

A Marconi AD 560 doppler navigation system was installed in the aircraft to assist in flying lines accurately.

Ground speed was measured to an accuracy of ± 0.5 per cent and aircraft drift to ± 1°. The ground speed of the aircraft was integrated with respect to time to give a continuous indication of the distance travelled along track and across track. The along track distances in kilometres were displayed on both analogue records, whilst the across track readings with an FSD of 25 km were displayed on the same record as the barometric altimeter.

5. EQUIPMENT TESTS AND SPECIFICATIONS

5.1 AIRBORNE MAGNETOMETER

The CENG MPPE 101 magnetometer has a sensitivity of 0.01 nT when flying under normal conditions. In Somalia, severe turbulence occurred on many sorties. As a consequence, the magnetometer noise envelope was generally not more than 0.2 nT, though in the worst conditions it occasionally exceeded 0.5 nT.

5.2 GROUND MAGNETOMETER

The CENG ground magnetometer had a sensitivity better than 1.0 nT which enabled all diurnal effects to be easily observed.

The orginal contract specification stated that when the curvilinear variations in the total field occur repeatedly for five minutes or more and have amplitudes greater than 5 nT within a five minute period, the corresponding lines would be reflown. However, in some cases this did not prove practical due to a shortage of aircraft fuel. The data had to be carefully checked and compared with the airborne records prior to acceptance. (See 7.1.5.).

5.3 ALTIMETER

The barometric altimeter calibration was checked daily at the airport.

6. ON-SITE DATA COMPILATION

A data compilation office and photographic dark room were set up at the operational base in Hargeisa. Here the 35mm tracking film was developed and the flight path recovered onto 1:100,000 coloured topographic maps and 1:60,000 photomosaics.

7. LABORATORY DATA COMPILATION AND PRESENTATION

7.1 COMPUTER PROCESSES

7.1.1 Navigation Files

The 1:100,000 navigation maps were digitised and the flight and tie line positions converted to UTM coordinates using the Krasovski spheroid on a Gaussian projection. These data were stored on disk files. Aircraft speed checks then ensured that the navigation files were free of major errors.

7.1.2 Field Data Tapes

Both airborne and ground magnetic data were read from the field tapes, verified, edited and merged with the navigation information to form a set of random access disk files.

7.1.3 Filtering

Both sets of magnetic data were passed through a de-spiking filter to remove instrument noise, then the airborne data were filtered with the intention of suppressing frequencies between 0.5 and 0.08 cycles per data interval. These correspond to the Nyquist frequency and that of a point pole at a distance of 500 m below the magnetometer sensor respectively. This latter is assumed to be the highest pertaining to any geological source that would be detected by the magnetometer configuration used for this survey. The frequency response of this filter is shown in Figure 8 and the equivalent space domain convolution filter is listed in Appendix C.

7.1.4 Regional Magnetic Field Correction

The airborne magnetic data was corrected for the regional field by subtracting the IGRF, Epoch 1981.7 (Ref. IAGA, 1976).

7.1.5 Diurnal Control

Under normal survey conditions, diurnal control can be affected by the standard L-T (line minus tie) control method. This is carried out by a systematic comparison of the TI values at all flight and tie line intersections. The small residual errors are distributed by fitting the TI differences at the intersections around successive loops of flight and tie lines, thus resulting in minor residual closure errors. Where the diurnal variations were in excess of contract specifications, a careful comparison of ground and airborne magnetic records was carried out, and those line segments in which data quality was excessively degraded by diurnal variations were excluded from the control process. A total of 40 line kilometres of data was rejected for this reason.

7.1.6 Horizontal Gradient Calculation

The horizontal gradient data was derived from the TI (airborne) data produced by the operations described in Sections 7.1.3 and 7.1.4 by means of a five point operator. The filter coefficients are given in Appendix C. The horizontal gradient was further filtered to remove any anomalies of wavelength less than 16 data intervals.

7.2 DATA PRESENTATION

The geophysical data are presented as follows:

(i) Eleven map sheets showing the aircraft's flight track with the coastline and concession boundary at 1:100,000 scale.

(ii) Eleven map sheets of total magnetic intensity contours, computer drawn at 1:100,000 scale, with flight track, coastline and concession boundary in subdued form.

(iii) Eleven sheets of magnetic interpretation of 1:100,000 scale showing magnetic basement isobaths and major magnetic features e.g. faults, intrusives, and intrabasement and intrasedimentary features. Again presented with flight tracks, coastline and concession boundary in subdued form.

(iv) Two map sheets at 1:250,000 scale showing the aircraft flight track, and the coastline and concession boundary.

(v) Two map sheets of total magnetic intensity at 1:250,000 scale.

(vi) Two map sheets of magnetic interpretation at 1:250,000 scale.

(vii) Computer plotted CALCOMP profiles for all flight and tie lines at 1:100,000 horizontal scale showing the following data:

(a)	ground clearance	scale 50 m/cm
(b)	total intensity (ground)	scale 5 nT/cm
(c)	total intensity (air)	scales 5nT/cm and 25nT/cm
(d)	horizontal gradient	scale 0.1nT/sec/cm

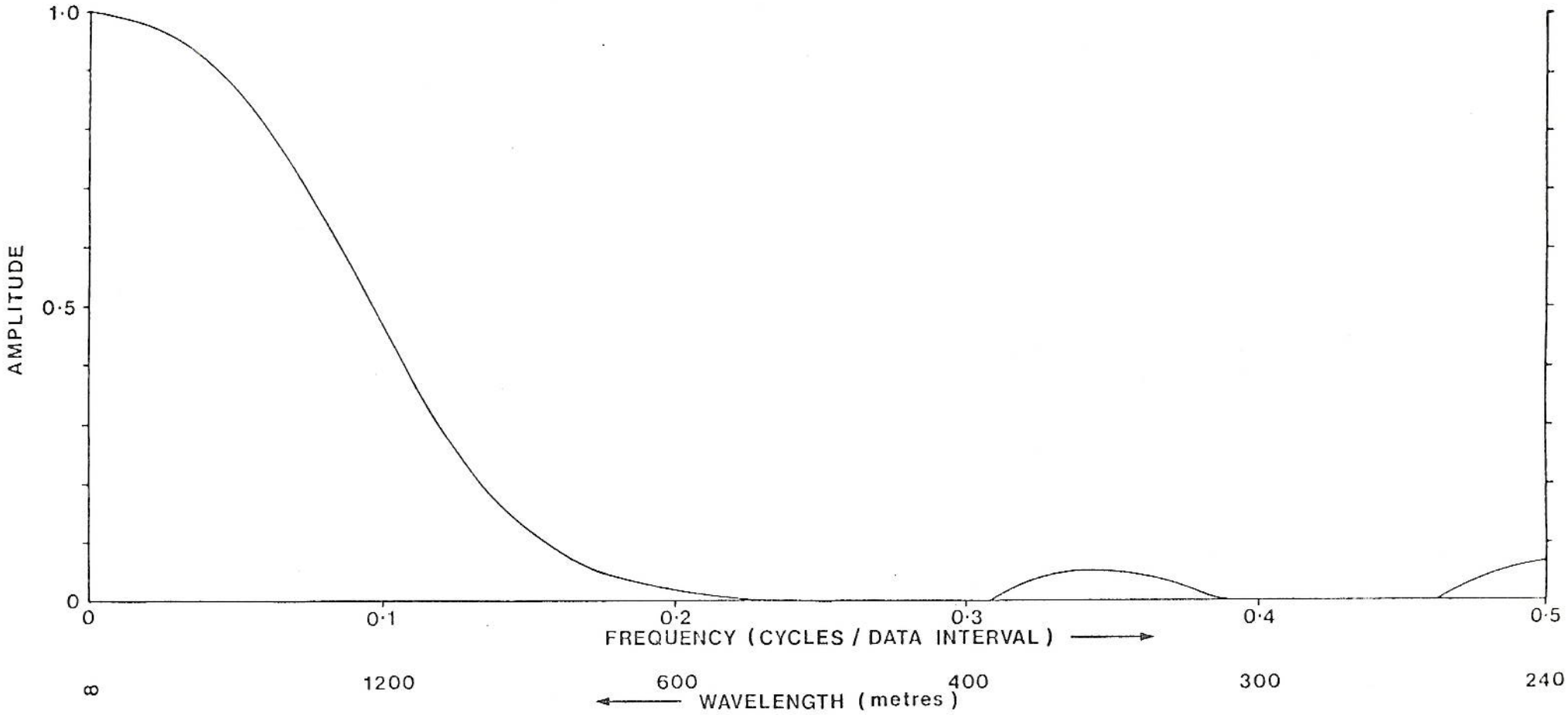

FREQUENCY RESPONSE OF SMOOTHING FILTER APPLIED TO AIRBORNE DATA

FIGURE 8

8. MATERIALS SUPPLIED TO THE CLIENT

(a) All original data acquired during the survey.

(b) All materials utilised for the preparation and carrying out of the survey (maps, flight logs, etc.).

(c) All relevant information acquired in connection with the performance of the work.

(d) An archive tape, whose format is given in Appendix A.

Final maps and reports supplied to the client are as follows:

(i) One transparency and 4 paper copies of total magnetic intensity maps.

(ii) One transparency and 4 paper copies of interpretation maps.

(iii) 4 copies of the interpretation and operations report.

APPENDIX A

DATA TAPE FORMATS

APPENDIX A

DATA TAPE FORMATS

1. AIRBORNE TAPE FORMAT

Specification: 9 track NRZ1. 800 BPI. ASCII code (not EBCIDIC)
Block length 990 characters. Scan length 99 characters.
Tape length 600 feet.

Scan Format:

Character	Description	
1	Y	Year
2	Year x 10^1	
3	Year x 10^0	
4	D	Day of Year
5	Day x 10^2	
6	Day x 10^1	
7	Day x 10^0	
8	H	Time of Day
9	Hours x 10^1	
10	Hours x 10^0	
11	M	
12	Minutes x 10^1	
13	Minutes x 10^0	
14	S	
15	Seconds x 10^1	
16	Seconds x 10^0	
17	F	Header I.E. Manually keyed in information.
18		
19		
20		
21		
thru to		
28		
29	Fiducial x 10^5	Scan Counter, (1 second increments) Camera Counter, and Analog event mark number
30	Fiducial x 10^4	
31	Fiducial x 10^3	
32	Fiducial x 10^2	
33	Fiducial x 10^1	
34	Magnetometer x 8^7	CENG Magnetometer Total Field 0.01 Gamma Units in Octal Code
35	Magnetometer x 8^8	
36	Magnetometer x 8^5	
37	Magnetometer x 8^4	
38	Magnetometer x 8^3	
39	Magnetometer x 8^2	
40	Magnetometer x 8^1	
41	Magnetometer x 8^0	- (0.01 γ Digit)

cont'd/....2

Character	Description	
42 thru 81	Zero	
82	Barometric Deviation + or -	Barometric deviation in (1/10ths) feet above (i.e. +) or below (i.e. -) flight datum of .....AMSL
83	Barometric Deviation x 10^2	
84	Decimal Point (not relevant)	
85	Barometric Deviation x 10^1	
86	Barometric Deviation x 10^0	
87	Barometric Deviation x 10^{-1}	
88	Radar Altitude + or -	Radar altitude in feet
89	Radar Altitude x 10^3	
90	Decimal Point (not relevant)	
91	Radar Altitude x 10^2	
92	Radar Altitude x 10^1	
93	Radar Altitude x 10^0	
94	+ or -	Unused Analog. (reading near zero)
95	10^3	
96	Decimal Point	
97	10^2	
98	10^1	
99	10^0	

END OF SCAN

ARCHIVE TAPE FORMAT

Specification:- 9 Track 1600 BPI EBCDIC
96 Characters per scan, 21 scans per block.

Formats:- (i) Line Header given in 2(F12.5) and 9 (F8.0):-

-800
Line no.
Start time
Line type (1 = tie line, 0 = flight line)
Julian day
Direction in degrees
-800
-800
-800
-800
-800

(ii) Data records in 2(F12.5) and 9(F8.0)

Latitude (decimal degrees)
Longitude (decimal degrees)
X coordinate (Krasovski co-ords)
Y coordinate (Krasovski co-ords)
Fiducial at plotted point or -100
Barometric altitude deviation (feet)
Radar altimeter (feet)
Raw magnetic value (Air)in 0.01nT
Raw magnetic value (Ground) in 0.01nT
Controlled magnetic value in 0.01nT
Horizontal gradient in 0.01nT/sec

(iii) Trailer in 2(F12.5) and 9(F8.0)
-850 -850 (eleven times)

There are 2 files on the tape corresponding to the two zones of Krasovski spheroid used:-

(i) File 1 contains all data west of 48°E

(ii) File 2 contains all data east of 48°E

APPENDIX B

FLIGHT LINE INDEX

FLIGHT LINE INDEX

LINE NO	DIR	SORTIE	DATE	LINE NO	DIR	SORTIE	DATE
1/1	S	4	24. 7.81	27/1	S	6	27. 7.81
1/2	S	8	30. 7.81	27/2	S	8	30. 7.81
2/1	N	4	24. 7.81	28/1	N	8	30. 7.81
2/2	N	5	25. 7.81	28/2	S	16	16.10.81
3/1	S	4	24. 7.81	29/1	N	6	27. 7.81
3/2	S	5	25. 7.81	29/2	N	8	30. 7.81
4/1	N	4	24. 7.81	30/1	N	8	30. 7.81
4/2	N	5	25. 7.81	30/2	N	16	16.10.81
5/1	N	4	24. 7.81	31/1	S	8	30. 7.81
5/2	S	5	25. 7.81	31/2	S	16	16.10.81
6/1	N	2	18. 7.81	32/1	S	8	30. 7.81
6/2	N	5	25. 7.81	32/2	N	16	16.10.81
7/1	S	4	24. 7.81	33/1	S	8	30. 7.81
7/3	N	13	9.10.81	33/2	S	16	16.10.81
8/2	N	4	24. 7.81	34/1	N	8	30. 7.81
8/3	S	5	25. 7.81	34/2	N	16	16.10.81
9/1	S	2	18. 7.81	35/1	S	23	28.10.81
9/2	N	5	25. 7.81	36/1	S	14	11.10.81
10/1	S	4	24. 7.81	37/1	N	13	9.10.81
10/2	S	5	25. 7.81	38/1	S	13	9.10.81
11/1	N	4	24. 7.81	39/1	S	13	9.10.81
11/2	N	8	30. 7.81	40/1	N	13	9.10.81
12/1	S	4	24. 7.81	41/1	N	26	30.10.81
12/2	N	8	30. 7.81	42/1	S	14	11.10.81
13/1	N	4	24. 7.81	43/1	N	27	2.11.81
13/2	S	8	30. 7.81	44/1	S	27	2.11.81
14/1	S	4	24. 7.81	44/2	N	27	2.11.81
14/2	S	8	30. 7.81	45/1	N	27	2.11.81
15/1	N	4	24. 7.81	46/1	S	14	11.10.81
15/2	S	8	30. 7.81	47/1	S	27	2.11.81
16/1	S	4	24. 7.81	48/1	N	27	2.11.81
16/2	N	8	30. 7.81	49/1	S	27	2.11.81
17/1	N	8	30. 7.81	50/1	S	13	9.10.81
17/2	S	25	29.10.81	51/1	N	27	2.11.81
18/1	N	8	30. 7.81	52/1	S	13	9.10.81
18/2	S	16	16.10.81	53/1	S	27	2.11.81
19/1	S	8	30. 7.81	54/1	N	27	2.11.81
19/2	N	16	16.10.81	55/1	S	27	2.11.81
20/1	S	8	30. 7.81	56/1	N	27	2.11.81
20/2	S	16	16.10.81	57/1	S	27	2.11.81
21/1	S	6	27. 7.81	58/1	N	27	2.11.81
21/2	S	8	30. 7.81	59/1	S	27	2.11.81
22/1	N	8	30. 7.81	60/1	N	14	11.10.81
22/2	N	16	16.10.81	61/1	S	14	11.10.81
23/1	N	8	30. 7.81	62/1	S	36	13.11.81
23/2	S	16	16.10.81	63/1	N	36	13.11.81
24/1	N	8	30. 7.81	64/1	N	14	11.10.81
24/2	N	16	16.10.81	65/1	S	14	11.10.81
25/1	S	8	30. 7.81	66/1	N	15	13.10.81
25/2	S	16	16.10.81	67/1	S	36	13.11.81
26/1	S	8	30. 7.81	68/1	N	15	13.10.81
26/2	N	16	16.10.81	69/1	S	15	13.10.81

FLIGHT LINE INDEX

LINE NO	DIR	SORTIE	DATE	LINE NO	DIR	SORTIE	DATE
70/1	N	36	13.11.81	120/1	S	22	27.10.81
71/1	S	15	13.10.81	121/1	N	22	27.10.81
72/1	N	15	13.10.81	122/1	S	22	27.10.81
73/1	S	32	11.11.81	123/1	N	22	27.10.81
74/1	S	36	13.11.81	124/1	S	22	27.10.81
75/1	S	15	13.10.81	125/1	N	22	27.10.81
76/1	N	15	13.10.81	126/1	S	22	27.10.81
77/1	S	15	13.10.81	127/1	N	22	27.10.81
77/2	N	18	22.10.81	128/1	S	22	27.10.81
78/1	N	26	30.10.81	129/1	N	22	27.10.81
79/1	S	17	17.10.81	130/1	S	22	27.10.81
80/1	N	23	28.10.81	131/1	N	22	27.10.81
81/1	S	7	29. 7.81	132/1	S	22	27.10.81
82/1	N	7	29. 7.81	133/1	N	22	27.10.81
83/1	S	7	29. 7.81	134/1	S	22	27.10.81
84/1	N	7	29. 7.81	135/1	N	22	27.10.81
85/1	S	7	29. 7.81	136/1	S	22	27.10.81
86/1	N	7	29. 7.81	137/1	N	22	27.10.81
87/1	S	7	29. 7.81	138/1	S	22	27.10.81
88/1	N	7	29. 7.81	139/1	N	22	27.10.81
89/1	N	19	23.10.81	140/1	S	22	27.10.81
90/1	S	19	23.10.81	141/1	N	22	27.10.81
91/1	N	19	23.10.81	142/1	S	22	27.10.81
92/1	S	19	23.10.81	143/1	N	22	27.10.81
93/1	N	19	23.10.81	144/1	S	22	27.10.81
94/1	S	19	23.10.81	145/1	N	22	27.10.81
95/1	N	19	23.10.81	146/1	S	22	27.10.81
96/1	S	19	23.10.81	147/1	N	22	27.10.81
97/1	N	19	23.10.81	148/1	S	22	27.10.81
98/1	S	19	23.10.81	149/1	N	22	27.10.81
99/1	N	19	23.10.81	150/1	N	35	12.11.81
100/1	S	19	23.10.81	151/1	S	35	12.11.81
101/1	S	32	11.11.81	152/1	N	35	12.11.81
102/1	S	21	26.10.81	153/1	S	35	12.11.81
103/1	N	21	26.10.81	154/1	N	17	17.10.81
104/1	N	32	11.11.81	155/1	S	17	17.10.81
105/1	S	32	11.11.81	156/1	N	17	17.10.81
105/2	N	36	13.11.81	157/1	S	17	17.10.81
106/1	S	21	26.10.81	158/1	N	35	12.11.81
107/1	N	21	26.10.81	159/1	S	17	17.10.81
108/1	S	21	26.10.81	160/1	N	17	17.10.81
109/1	N	21	26.10.81	161/1	S	35	12.11.81
110/1	S	21	26.10.81	162/1	N	17	17.10.81
111/1	N	21	26.10.81	163/1	S	17	17.10.81
112/1	S	21	26.10.81	164/1	N	17	17.10.81
113/1	N	21	26.10.81	165/1	S	17	17.10.81
114/1	S	21	26.10.81	166/1	N	17	17.10.81
115/1	N	21	26.10.81	167/1	S	17	17.10.81
116/1	S	21	26.10.81	168/1	N	17	17.10.81
117/1	N	21	26.10.81	169/1	S	17	17.10.81
118/1	S	21	26.10.81	170/1	N	17	17.10.81
119/1	N	22	27.10.81	171/1	S	17	17.10.81

FLIGHT LINE INDEX

T/LINE NO	DIR	SORTIE	DATE
1001/1	E	7	29. 7.81
1001/2	E	7	29. 7.81
1001/3	W	21	26.10.81
1001/4	E	36	13.11.81
1002/1	W	7	29. 7.81
1002/2	W	7	29. 7.81
1002/3	E	21	26.10.81
1002/4	W	35	12.11.81
1003/1	E	20	25.10.81
1003/2	W	21	26.10.81
1003/3	E	26	30.10.81
1003/4	W	31	10.11.81
1004/1	E	21	26.10.81
1004/2	W	23	28.10.81
1004/3	E	31	10.11.81
1004/4	E	36	13.11.81
1005/1	E	22	27.10.81
1005/2	E	22	27.10.81
1005/3	E	22	27.10.81
1005/4	W	26	30.10.81
1005/5	E	36	13.11.81
1006/1	E	23	28.10.81
1006/2	E	23	28.10.81
1006/3	W	26	30.10.81
1006/4	E	26	30.10.81
1007/1	W	26	30.10.81
1007/2	W	26	30.10.81
1007/3	E	36	13.11.81
1008/1	E	26	30.10.81
1008/2	E	26	30.10.81
1008/3	E	33	12.11.81
1008/4	W	35	12.11.81
1009/1	W	23	28.10.81
1009/2	W	25	29.10.81
1009/3	W	25	29.10.81
1009/4	E	32	11.11.81
1010/1	E	4	24. 7.81
1010/2	E	23	28.10.81
1010/3	E	25	29.10.81
1010/4	E	26	30.10.81
1010/5	W	32	11.11.81
1011/1	W	4	24. 7.81
1011/2	W	23	28.10.81
1011/3	E	26	30.10.81
1011/4	E	32	11.11.81
1012/1	E	4	24. 7.81
1012/2	E	23	28.10.81
1012/3	W	26	30.10.81
1012/4	W	36	13.11.81
1013/1	E	23	28.10.81
1013/2	W	23	28.10.81
1013/3	W	23	28.10.81
1014/1	W	21	26.10.81
1014/2	W	21	26.10.81
1014/3	W	23	28.10.81
1015/1	E	23	28.10.81
1015/2	W	23	28.10.81
1018/1	E	22	27.10.81
1019/1	E	33	12.11.81
1020/1	W	35	12.11.81
1021/1	W	17	17.10.81
1021/2	E	35	12.11.81
1022/1	W	35	12.11.81
1023/1	E	35	12.11.81
1024/1	W	4	24. 7.81
1025/1	SW	23	28.10.81
1026/1	NE	23	28.10.81
1027/1	SE	23	28.10.81
1028/1	SE	23	28.10.81
1029/1	SW	35	12.11.81
1030/2	W	35	12.11.81
1031/1	SE	17	17.10.81
1032/1	E	35	12.11.81
1033/1	SW	21	26.10.81

APPENDIX C

FILTER INFORMATION

APPENDIX C
FILTER INFORMATION

1. The airborne magnetic data was filtered using a 1 dimensional 15 coefficient convolution filter, the coefficients being as follows:

- 0.0187	
0.0093	
0.000	
0.0280	
0.0748	
0.1308	
0.1776	
0.1963	Central value
0.1776	
0.1308	
0.0748	
0.0280	
0.000	
0.0093	
- 0.0187	

The frequency response for this filter is shown in Figure 8.

2. The horizontal gradient filter was computed using the following algorithm:

$$\left(\frac{dT}{dx}\right)_{x_o} = \frac{1}{12}\left[T(x_o - 2) - 8T(x_o - 1) + 8T(x_o + 1) - T(x_o + 2)\right]$$

where: x_o = fiducial at which the gradient is calculated
$T(x_o-2)$ = TI, two fiducials before x_o
$T(x_o+1)$ = TI, one fiducial after x_o
The other terms are similarly defined.

The horizontal gradient is in units of nT per data interval and can be converted to nT/m by dividing the distance covered in one fiducial interval (i.e. approx 65m). The above expression is exact for any polynomial of degree four or less.

In practice this algorithm was converted to a five coefficient convolution filter with coefficients:

0.08333	
- 0.66667	
0.0000	- Central value
0.66667	
- 0.08333	

APPENDIX D

SAMPLE ANALOGUE RECORDS

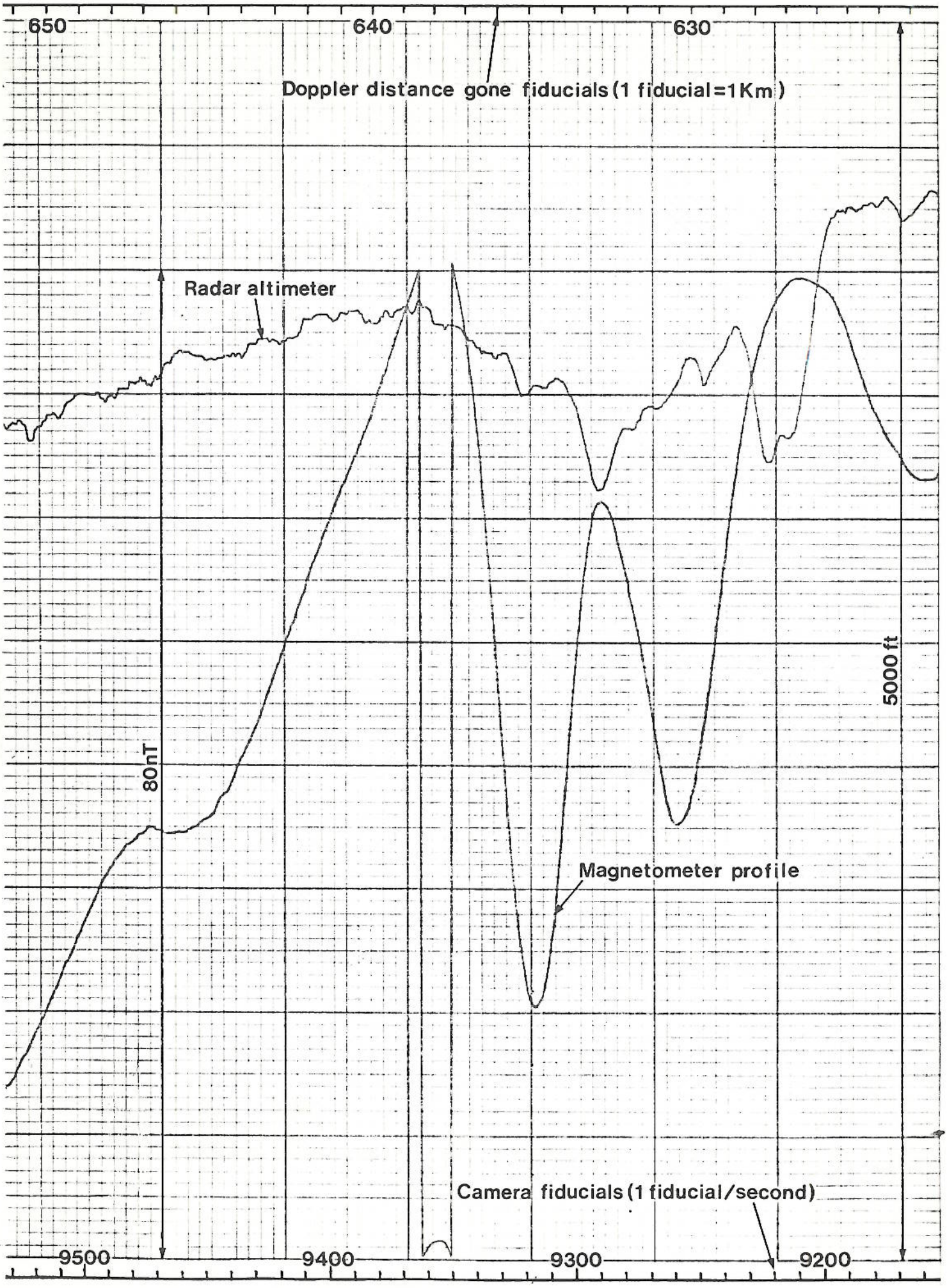

SAMPLE ANALOGUE RECORD

CENG Magnetometer and radar altimeter

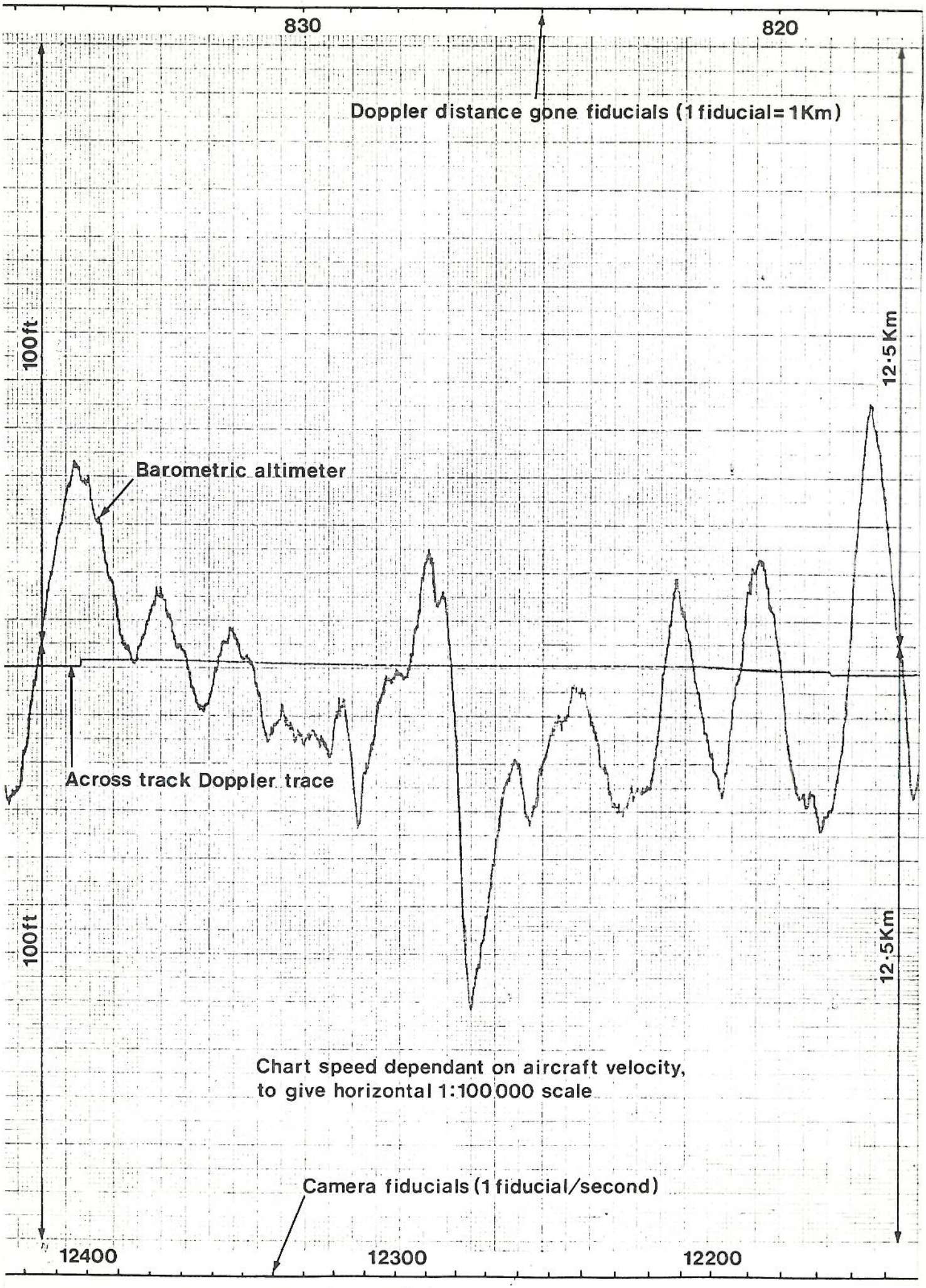

ANALOGUE RECORD

Barometric altimeter and Doppler